

CrossMark  
click for updatesCite this: *Chem. Sci.*, 2016, 7, 4059Regioselective phenylene-fusion reactions of Ni(II)-porphyrins controlled by an electron-withdrawing *meso*-substituent†Norihito Fukui,<sup>a</sup> Seung-Kyu Lee,<sup>b</sup> Kenichi Kato,<sup>a</sup> Daiki Shimizu,<sup>a</sup> Takayuki Tanaka,<sup>a</sup> Sangsu Lee,<sup>b</sup> Hideki Yorimitsu,<sup>\*a</sup> Dongho Kim<sup>\*b</sup> and Atsuhiko Osuka<sup>\*a</sup>

Oxidation of 10,15,20-triaryl Ni(II)-porphyrins bearing an electron-withdrawing substituent at the 5-position with DDQ and FeCl<sub>3</sub> gave 10,12- and 18,20-doubly phenylene-fused Ni(II)-porphyrins regioselectively. A doubly phenylene-fused *meso*-chloro porphyrin thus prepared was reductively coupled to give a *meso*–*meso* linked dimer, which was further converted to a quadruply phenylene-fused *meso*–*meso*, β–β, β–β triply linked Zn(II)-diporphyrin via inner-metal exchange followed by oxidation with DDQ and Sc(OTf)<sub>3</sub>. As compared to the usual *meso*–*meso*, β–β, β–β triply linked Zn(II)-diporphyrin, this π-extended porphyrin dyad exhibits a smaller HOMO–LUMO gap and a larger two-photon absorption cross-section.

Received 9th December 2015  
Accepted 1st March 2016

DOI: 10.1039/c5sc04748j

www.rsc.org/chemicalscience

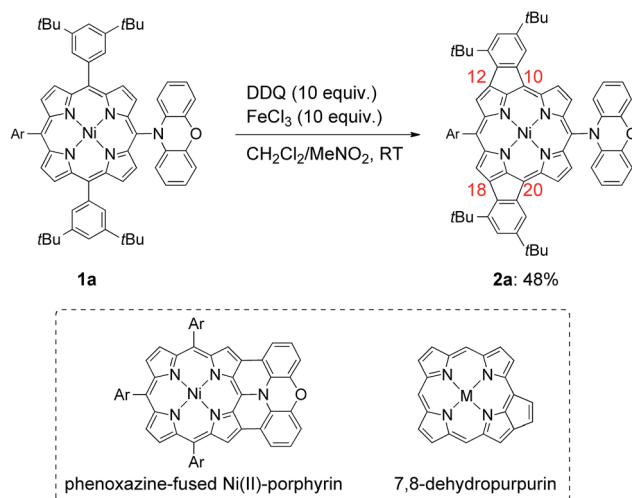
## Introduction

Porphyrins having extended π-electronic networks have been attracting considerable attention because of their applications such as organic semiconductors, near-infrared dyes, and nonlinear optical materials.<sup>1</sup> Among such π-extended porphyrins, 7,8-dehydropurpurins and their families, which have a double bond across the *meso*- and β-positions and thus contain a *peri*-fused five-membered ring directly onto the periphery, display largely altered absorption spectra, small HOMO–LUMO gaps, and weakened aromaticity.<sup>2–4</sup> These intriguing properties can be ascribed to their π-extended electronic networks involving a pseudo 20π-antiaromatic electronic circuit.

Recently, we reported that the oxidation of *meso*-phenoxazine-substituted Ni(II)-porphyrin **1a** with 2,3-dichloro-5,6-dicyano-*p*-benzoquinone (DDQ) and FeCl<sub>3</sub> unexpectedly gave doubly 10,12- and 18,20-phenylene-fused Ni(II)-porphyrin **2a** instead of phenoxazine-fused Ni(II)-porphyrin (Scheme 1).<sup>5</sup> Doubly phenylene-fused porphyrins such as **2a** are attractive pigments in view of altered optical and electronic properties as compared with mono phenylene-fused 7,8-dehydropurpurin derivatives. In addition, their symmetric structures are suitable for further oligomerizations and functionalizations. Despite

these potentials, the mechanism and scope of this double fusion reaction is not well understood.

Phenylene-fused 7,8-dehydropurpurins have been often prepared by Pd-catalyzed cyclizations via C–H activations of *meso*-(2-haloaryl)-substituted porphyrins or β-bromo-*meso*-aryl-substituted porphyrins.<sup>2</sup> In contrast, syntheses of phenylene-fused 7,8-dehydropurpurins upon oxidation have remained rather rare.<sup>4</sup> In this sense, the formation of **2a** is interesting and thus worth understanding further. In addition, the observed regioselectivity looks curious, considering that seven regioisomers are possible for doubly fusion products (ESI, Scheme S1†). In the oxidation of **1a**, the first oxidation at 0.34 V



Scheme 1 Synthesis of 10,12- and 18,20-phenylene-fused *meso*-phenoxazino Ni(II)-porphyrin **2a**, and structures of phenoxazine-fused porphyrin and 7,8-dehydropurpurin. Ar = 3,5-di-*tert*-butylphenyl.

<sup>a</sup>Department of Chemistry, Graduate School of Science, Kyoto University, Sakyo-ku, Kyoto 606-8502, Japan. E-mail: yori@kuchem.kyoto-u.ac.jp; osuka@kuchem.kyoto-u.ac.jp

<sup>b</sup>Spectroscopy Laboratory of Functional π-Electronic Systems, Department of Chemistry, Yonsei University, Seoul 120-749, Korea. E-mail: dongho@yonsei.ac.kr

† Electronic supplementary information (ESI) available. CCDC 1433486–1433489. For ESI and crystallographic data in CIF or other electronic format see DOI: 10.1039/c5sc04748j

(vs.  $\text{Fc}/\text{Fc}^+$ ) should occur at the *meso*-phenoxazine group, since it is easier to oxidize than the  $\text{Ni(II)}$ -porphyrin core.<sup>5</sup> We thought that the one-electron oxidized phenoxazine moiety might serve just as an electron-withdrawing group to the  $\text{Ni(II)}$ -porphyrin, helping the regioselective fusion reactions at the 12- and 18-positions. In order to check this postulate, we examined the oxidative fusion reactions of  $\text{Ni(II)}$ -porphyrins bearing an electron-withdrawing substituent at the 5-position.

## Results and discussion

### Oxidative fusion reactions of *meso*-functionalized porphyrins

Oxidative fusion reactions of porphyrins **1b–f** were examined with 10 equivalents of DDQ and  $\text{FeCl}_3$  in a mixture of  $\text{CH}_2\text{Cl}_2$  and  $\text{MeNO}_2$  (Scheme 2). Electron-rich substrate **1b<sup>e</sup>** was readily decomposed under these conditions. Weakly electron-deficient porphyrins **1c** and **1d** gave complicated mixtures consisting of various fused isomers. More electron-deficient 5-nitroporphyrin **1e** and 5-diphenylphosphinylporphyrin **1f** afforded the corresponding doubly phenylene-fused porphyrins **2e** and **2f** regioselectively in 29 and 61% yields, respectively, while singly phenylene-fused porphyrin **3** was isolated as a side product in 18% yield in the reaction of **1e**. The structures of **2e**, **2f** and **3** were all unambiguously determined by X-ray diffraction analyses (Fig. 1).<sup>8</sup> In **2e** and **2f**, the aryl groups at the 10- and 20-positions were fused onto the porphyrin periphery, as is the case of **2a**. The preferential formations of **2e** and **2f** suggest that a strongly electron-withdrawing *meso*-substituent plays an important role in the regioselective fusion reactions.

### Investigation into the regioselectivity

Recently, Kadish and Gryko *et al.* proposed, on the basis of detailed electrochemical studies, that the oxidative fusion reaction of *meso*-naphthylporphyrin might occur *via* one-electron oxidations of both the porphyrin and naphthalene moieties followed by an intramolecular radical–radical coupling between generated porphyrinyl radical cation and naphthyl

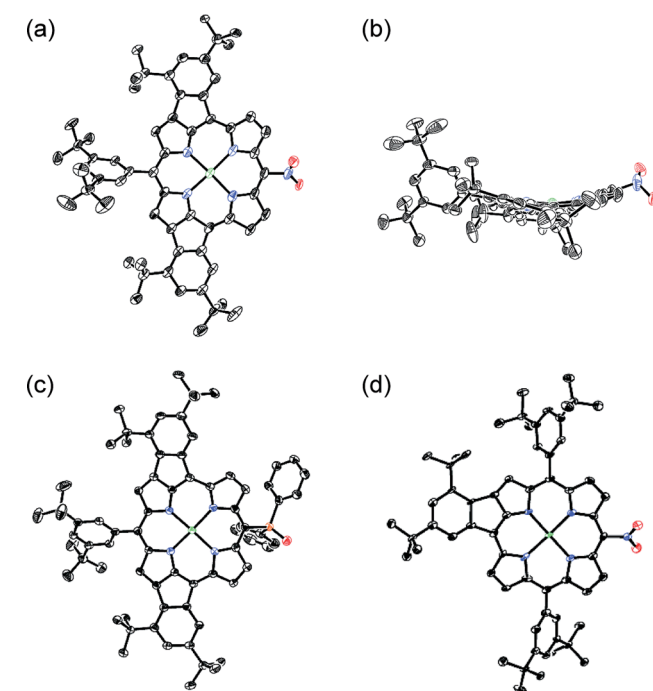
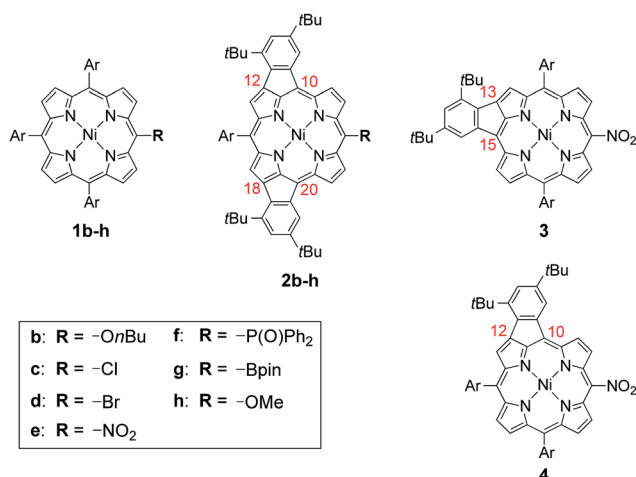


Fig. 1 X-Ray crystal structures. (a) Top view and (b) side view of **2e**, (c) top view of **2f**, and (d) top view of **3**. Thermal ellipsoids are drawn at the 50% probability level. Solvent molecules and all hydrogen atoms are omitted for clarity.

radical cation.<sup>9,10</sup> In this intramolecular radical coupling mechanism, the spin density of the porphyrinyl radical cation should govern the selectivity.

To find a clue about the regioselectivity, we performed density functional theory (DFT) calculations.<sup>11</sup> Spin density maps of radical cations of **1e** and **1h** were calculated at the B3LYP/6-311G\* level using the *Gaussian 09* package<sup>12</sup> (Fig. 2a and b). 5-Substituted porphyrins possess three possible reaction sites to connect with *meso*-phenyl groups, namely 8-, 12- and 13-positions. In the case of 5-nitroporphyrin **1e**, the largest spin density value of 0.052 was calculated at the 12-position. On the other hand, in the case of 5-methoxyporphyrin **1h**, spin density values at the possible reaction sites are almost similar. These results accord with our experimental observation that a strong electron-withdrawing group promoted the regioselective fusion of *meso*-phenyl groups at the 12- and 18-positions. Moreover, we



Scheme 2 Structures of **1b–h**, **2b–h**, **3** and **4**. Ar = 3,5-di-*tert*-butylphenyl.

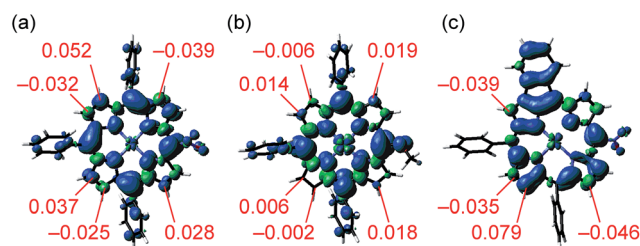


Fig. 2 Total spin density of radical cations of (a) **1e**, (b) **1h** and (c) **4** obtained by DFT calculations at the B3LYP/6-311G\* level (isovalue: 0.001). *tert*-Butyl groups were replaced with hydrogen atoms to simplify the calculations.



also calculated the spin density of singly 10,12-phenylene-fused 5-nitroporphyrin **4**, which is a possible intermediate to provide doubly 10,12- and 18,20-phenylene-fused porphyrin **2e** (Fig. 2c). Curiously, compared to the case of radical cation of **1e**, the difference of spin density values between 12- and other positions became more distinguishable, which might imply that electronic perturbation by the fused phenylene unit urged the opposite *meso*-phenyl group to react with the 18-position.

Another possible mechanism, nucleophilic attack of the peripheral aryl group to the cationic porphyrin core, has been proposed.<sup>13</sup> According to this mechanism, we also performed DFT calculations of dications of **1e** and **1h**. However, both in the case of radical cations and dications of **1e** and **1h**, the obtained molecular orbitals or charge distributions showed no clear difference at the 8-, 12- and 13-positions to explain the regioselectivity (ESI, Fig. S46–S50†). From the point of view of these calculations, an intramolecular radical–radical coupling mechanism seems plausible for our phenylene-fusion reactions.

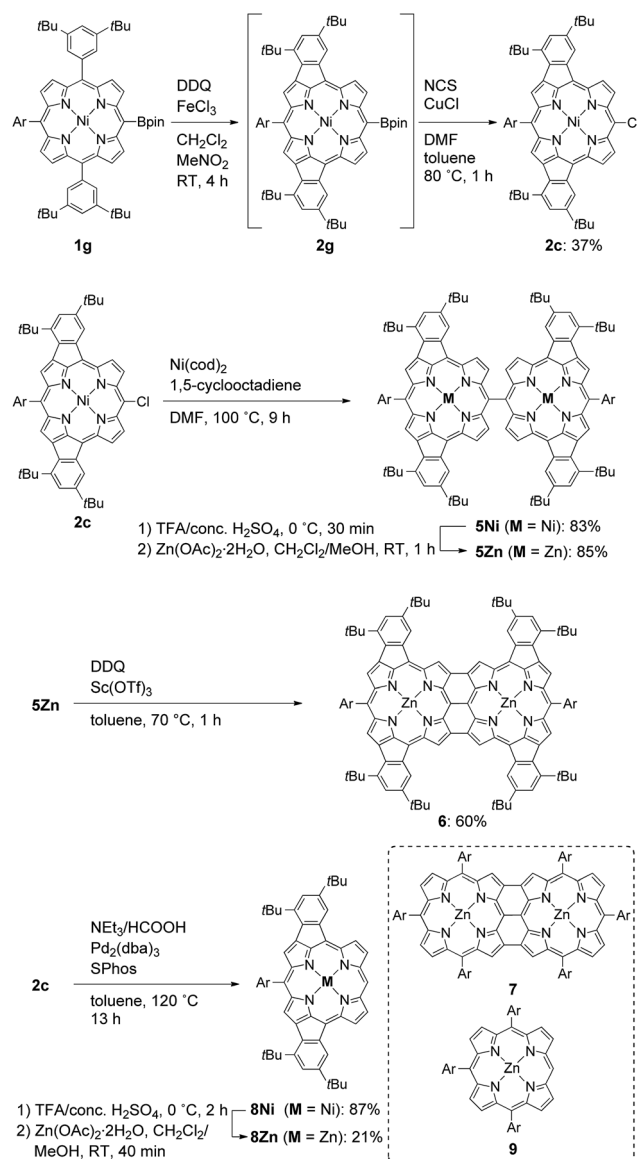
It is of note to mention that numerous studies have proven that electron-rich aromatic compounds easily undergo the oxidative fusion reactions.<sup>13</sup> In the case of small aromatic compounds, the presence of an electron-withdrawing group decreases the HOMO level to prevent the initial oxidation. On the other hand, for large aromatic compounds including porphyrin, such a decrease of the HOMO will be too negligible to stop the oxidative fusion reactions. In our reactions, electron-withdrawing groups might strongly reorganize the overall electron-density to make the 12-position relatively reactive.

### Synthesis of a *meso*-chloro doubly phenylene-fused Ni(II)-porphyrin

In the next step, we chose a pinacolatoboryl group as an interconvertible electron-withdrawing substituent (Scheme 3). The reaction of 5-pinacolatoborylporphyrin **1g**<sup>14</sup> afforded doubly phenylene-fused porphyrin **2g** with partial production of *meso*-chloroporphyrin **2c**. Thus, we subjected this crude reaction mixture of **2c** and **2g** directly to Cu-mediated chlorination conditions,<sup>15</sup> which allowed for isolation of **2c** in 37% yield. It is of note that **2c** is a useful precursor for further fabrications but is inaccessible through the direct oxidation of **1c**.

### Synthesis of a quadruply phenylene-fused *meso-meso*, $\beta$ - $\beta$ , $\beta$ - $\beta$ triply linked Zn(II)-diporphyrin

With **2c** in hand, we envisioned the synthesis of quadruply phenylene-fused *meso-meso*,  $\beta$ - $\beta$ ,  $\beta$ - $\beta$  triply linked Zn(II)-diporphyrin **6** as a new  $\pi$ -extended *meso-meso*,  $\beta$ - $\beta$ ,  $\beta$ - $\beta$  triply linked porphyrin dyad. The synthetic route to dimer **6** is shown in Scheme 3. Ni(0)-mediated reductive homo-coupling<sup>16</sup> of **2c** furnished *meso-meso* linked diporphyrin **5Ni** in 83% yield. Removal of the central nickel atoms of **5Ni** with concentrated sulfuric acid in trifluoroacetic acid (TFA) proceeded cleanly at 0 °C, and subsequent zincation afforded **5Zn** in 85% yield in two steps. Finally, the oxidative fusion reaction of **5Zn** with DDQ and Sc(OTf)<sub>3</sub><sup>17</sup> gave **6** in 60% yield. Doubly phenylene-fused Zn(II)-porphyrin monomer **8Zn** was synthesized as a reference



**Scheme 3** Synthesis of quadruply phenylene-fused *meso-meso*,  $\beta$ - $\beta$ ,  $\beta$ - $\beta$  triply linked Zn(II)-diporphyrin **6** and structure of *meso-meso*,  $\beta$ - $\beta$ ,  $\beta$ - $\beta$  triply linked Zn(II)-diporphyrin **7**. Ar = 3,5-di-*tert*-butylphenyl, NCS = *N*-chlorosuccinimide, cod = 1,5-cyclooctadiene, dba = dibenzylideneacetone, SPhos = 2-(2',6'-dimethoxybiphenyl)dicyclohexylphosphine.

compound by dechlorination of **2c** followed by removal of the nickel and zinc-metalation.

The atmospheric pressure chemical ionization time-of-flight mass spectra of **5Zn** and **6** displayed the parent ion peaks at 1862.9249 (calcd for C<sub>124</sub>H<sub>134</sub>N<sub>8</sub><sup>64</sup>Zn<sub>2</sub>, *m/z* 1862.9320 [M]<sup>−</sup>) and 1858.8967 (calcd for C<sub>124</sub>H<sub>130</sub>N<sub>8</sub><sup>64</sup>Zn<sub>2</sub>, *m/z* 1858.9007 [M]<sup>−</sup>), respectively, indicating that four hydrogen atoms were removed during the oxidative fusion reaction from **5Zn** to **6**. The <sup>1</sup>H NMR spectrum of **6** in pyridine-*d*<sub>5</sub> showed six signals at 8.19, 8.06, 8.00, 7.86, 7.33 and 7.29 ppm in the aromatic region. The structure of **6** has been revealed by X-ray crystallographic analysis to be fairly coplanar with a small mean plane deviation (MPD) of 0.102 Å (Fig. 3).<sup>18,19</sup> The C<sub>*meso*</sub>–C<sub>*meso*</sub> bond length is

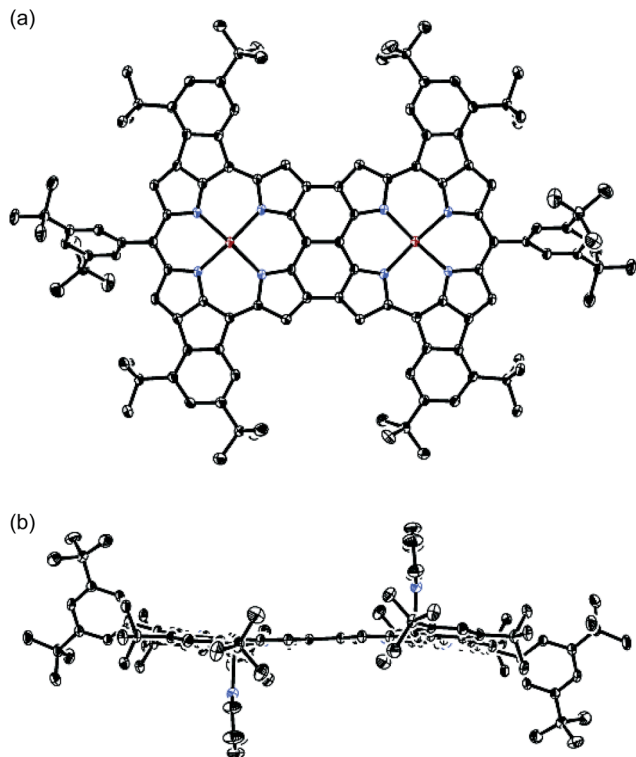


Fig. 3 X-Ray crystal structure of **6**. (a) Top view and (b) side view. Thermal ellipsoids are drawn at the 50% probability level. Solvent molecules and all hydrogen atoms are omitted for clarity. In the top view, pyridine ligands on the central Zn atoms are also omitted for clarity.

1.489(3) Å, and the two C<sub>β</sub>–C<sub>β</sub> bond lengths are both 1.442(3) Å. These structural features are similar to those of previously reported porphyrin dyad **7**.<sup>17f</sup>

### UV/vis absorption spectra and density functional theory calculations

The UV/vis/NIR absorption spectra of **8Zn**, **5Zn**, **6** and **7** are shown in Fig. 4. CH<sub>2</sub>Cl<sub>2</sub> containing 1% of pyridine was employed as a solvent to increase the solubility of these

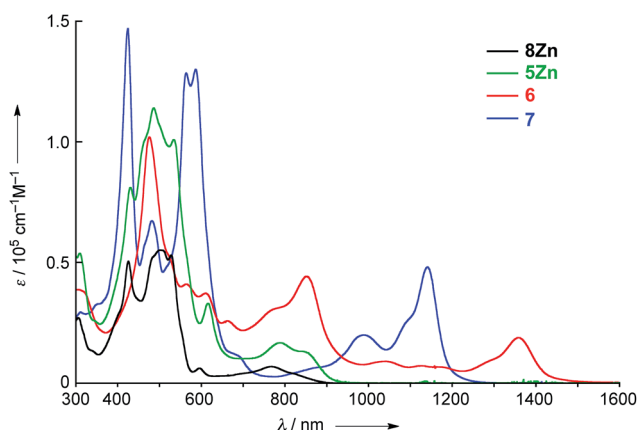


Fig. 4 UV/vis/NIR absorption spectra of **8Zn**, **5Zn**, **6** and **7** in CH<sub>2</sub>Cl<sub>2</sub> containing 1% pyridine.  $\epsilon$  = molar extinction coefficient.

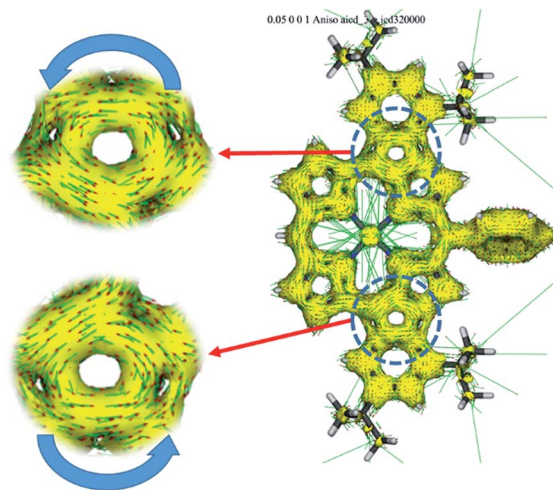


Fig. 5 ACID plot for **8Zn** at an isosurface value of 0.05 at the B3LYP/6-31(d) level.

compounds by the axial coordination of pyridine to the central Zn atom. As compared with normal Zn(II)-porphyrins, doubly phenylene-fused porphyrin **8Zn** exhibits a red-shifted and broad absorption spectrum, probably due to the  $\pi$ -extension and pseudo  $20\pi$ -antiaromatic contribution. In line with this, the anisotropy of the induced current density (ACID) plot<sup>20</sup> around the fused five-membered ring of **8Zn** was calculated to be counterclockwise (Fig. 5). In addition, the NICS(0) value<sup>21</sup> at the center of the fused five-membered ring was calculated to be a large positive value of +17.0 at the B3LYP/6-31(d) level using the *Gaussian 09* package.<sup>12</sup> The *meso-meso* linked dimer **5Zn** shows an absorption spectrum which is slightly red-shifted, but otherwise similar to that of **8Zn**, indicating small electronic interaction between the two doubly phenylene-fused porphyrin units. In contrast, the absorption spectrum of **6** is strongly altered and red-shifted, showing bands at 476, 851 and 1358 nm. The Q-like band at 1358 nm in **6** is red-shifted by 217 nm ( $1.4 \times 10^3 \text{ cm}^{-1}$ ) as compared with that of **7** at 1141 nm, as an indication of a more  $\pi$ -extended network in **6**. Interestingly, **6** shows a characteristic absorption band at 851 nm, while such a band was not observed in other  $\pi$ -extended *meso-meso*,  $\beta$ - $\beta$ ,  $\beta$ - $\beta$  triply linked diporphyrins.<sup>22</sup>

Time-dependent density functional theory (TD-DFT) calculations on **6** and **7** were performed at the B3LYP/6-31G\*(C,H,N) + LANL2DZ(Zn) level using *Gaussian 09* package<sup>12</sup> (See ESI). The TD-DFT calculations roughly reproduced the absorption spectra of **6** and **7**. The calculations suggested that the absorption at 851 nm in **6** is mainly ascribed to the transition from the HOMO–1 to LUMO+1. The same transition was calculated around 600 nm for **7**. This difference may be ascribed to the largely stabilized LUMO+1 in **6** through the interaction with the fused five-membered rings.

### Electrochemical properties

The electrochemical properties of **8Zn**, **5Zn**, **6** and **7** were studied by cyclic voltammetry (CV) and differential pulse





voltammetry (DPV) in  $\text{CH}_2\text{Cl}_2$  containing 1% pyridine with 0.1 M  $n\text{Bu}_4\text{NPF}_6$  as a supporting electrolyte (Fig. 6). Doubly phenylene-fused porphyrin monomer **8Zn** showed three reversible oxidation waves at 0.16, 0.37 and 0.63 V, and two reversible reduction waves at  $-1.53$  and  $-2.02$  V. The electrochemical HOMO–LUMO gap  $\Delta E$  ( $E_{\text{ox1}}^{1/2} - E_{\text{red1}}^{1/2}$ ) of **8Zn** was calculated to be 1.69 eV. This  $\Delta E$  value is much smaller than that of triaryl Zn(II)-porphyrin **9** (2.22 eV),<sup>23</sup> which can be ascribed to the effective  $\pi$ -extension caused by the pseudo  $20\pi$ -antiaromatic contribution.

The corresponding *meso-meso* linked dimer **5Zn** displayed four reversible oxidation waves at 0.13, 0.30, 0.51 and 0.59 V, and four reversible reduction waves at  $-1.45$ ,  $-1.58$ ,  $-2.04$  and  $-2.11$  V. The first and second reduction waves can be assigned as split first reduction waves (one electron per porphyrin unit) as judged from the results of other electronically coupled diporphyrins.<sup>24</sup> The  $\Delta E$  value of **5Zn** was calculated to be 1.58 eV, which is very similar to that of **8Zn**, suggesting little electronic communication between the two phenylene-fused porphyrin units. On the other hand, quadruply phenylene-fused

*meso-meso*,  $\beta$ - $\beta$ ,  $\beta$ - $\beta$  triply linked Zn(II)-diporphyrin **6** showed remarkably perturbed potentials. **6** exhibited two reversible oxidation waves at  $-0.15$  and  $0.19$  V, and four reversible reduction waves at  $-1.10$ ,  $-1.35$ ,  $-1.79$  and  $-2.02$  V. Then, **7** showed two reversible oxidation waves at  $-0.13$  and  $0.27$  V, and two reversible reduction waves at  $-1.24$  and  $-1.45$  V. The first reduction potential of **6** showed a large positive shift of 0.14 V compared to that of **7**, while the first oxidation potential displayed a small negative shift of 0.02 V. The  $\Delta E$  value of **6** is calculated to be 0.95 V. It is apparently smaller than that of *meso-meso*,  $\beta$ - $\beta$ ,  $\beta$ - $\beta$  triply linked Zn(II)-diporphyrin **7** (1.11 eV), indicating the effective  $\pi$ -delocalization over the fused phenylene units. These results indicate that introduction of fused phenylene units is effective to enhance the electron-accepting property, which is in accord with the calculated molecular orbital diagrams of **6** and **7** (ESI, Fig. S41†). The obtained  $\Delta E$  values for **8Zn**, **5Zn**, **6** and **7** were almost close in value to the observed optical gaps.

### Femtosecond transient absorption measurements

Femtosecond transient absorption measurements were carried out for **8Zn**, **5Zn** and **6** in toluene containing 1% of pyridine (Fig. 7). Excitation wavelengths are 800 nm for **8Zn** and **5Zn**, and 1350 nm for **6**, which correspond to the lowest Q-like bands. All the compounds exhibit single exponential decay profiles of the ground-state-bleaching signals (4.0, 3.5 and 2.0 ps, respectively). Compound **7** shows a similar decay time of 4.5 ps.<sup>25</sup> The observed short  $S_1$ -state lifetime of **8Zn** may be ascribed to the pseudo  $20\pi$ -antiaromatic contribution of 7,8-dehydropurpurin-like structure<sup>2e</sup> and accelerated non-radiative relaxation associated the narrow

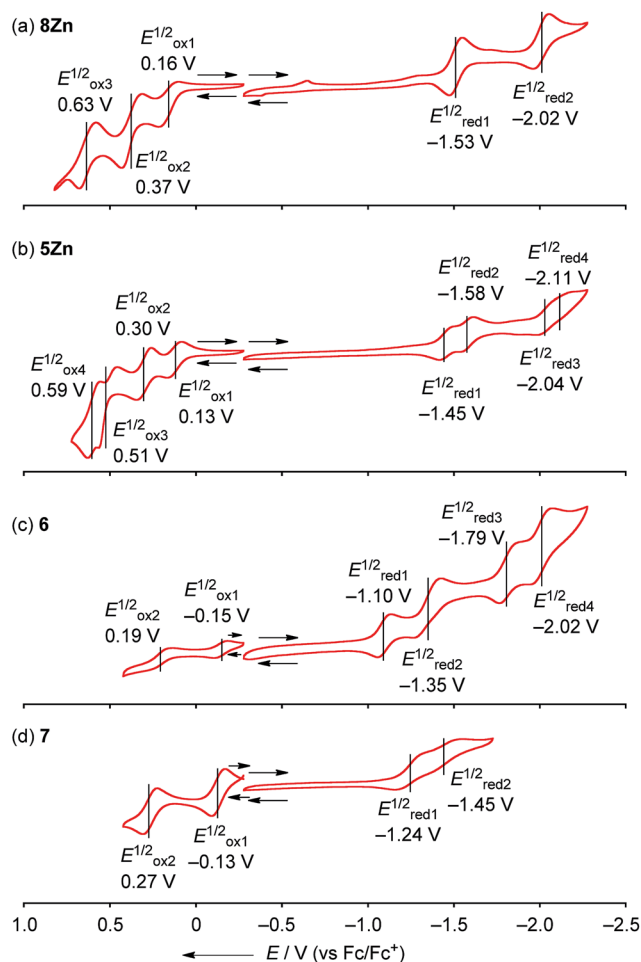


Fig. 6 Cyclic voltammograms of (a) **8Zn**, (b) **5Zn**, (c) **6** and (d) **7**. The redox potentials were measured by cyclic voltammetry in anhydrous  $\text{CH}_2\text{Cl}_2$  containing 1% pyridine with 0.1 M  $n\text{Bu}_4\text{NPF}_6$  as a supporting electrolyte, and  $\text{Ag}/\text{AgNO}_3$  as a reference electrode. Ferrocene/ferrocenium ion couple was used as an external reference.

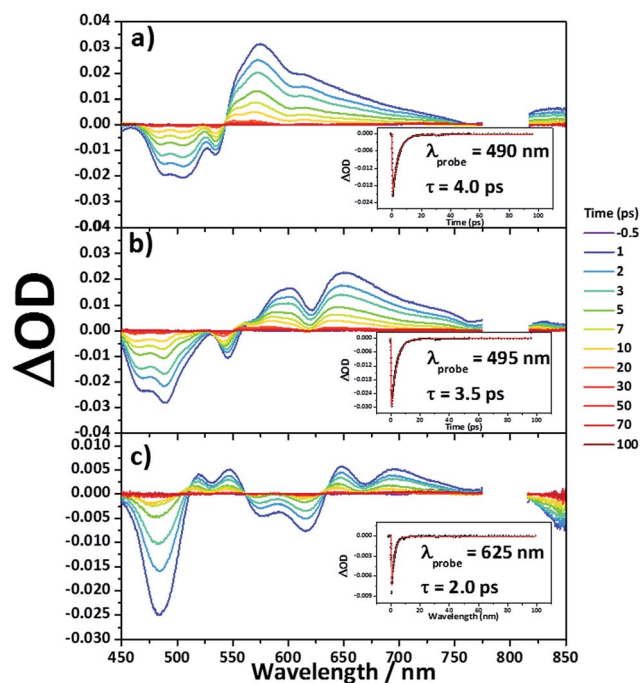


Fig. 7 Femtosecond transient absorption spectra and decay profiles (inset) of (a) **8Zn**, (b) **5Zn** and (c) **6** in toluene containing 1% of pyridine with photoexcitation at 800 nm (for **8Zn** and **5Zn**), and 1350 nm (for **6**).

energy gap. The decay constant of **5Zn** is very similar to that of **8Zn** due to small interaction between the two doubly phenylene-fused porphyrin cores. An observation that the  $S_1$ -state lifetime of **6** is shorter than that of **7** can be interpreted in terms of the reduced HOMO–LUMO gap arising from the extended  $\pi$ -conjugation and contribution of  $20\pi$ -antiaromaticity.<sup>26</sup>

## Two-photon absorption properties

Recently,  $\pi$ -conjugated organic molecules have attracted much attention as soft processable nonlinear optical materials in light of their possible applications such as for photodynamic therapy.<sup>27</sup> It has been demonstrated that  $\pi$ -extended porphyrins exhibit large nonlinear optical responses.<sup>1e,g,22d</sup> Therefore, two-

photon absorption (TPA) properties of **8Zn**, **5Zn**, **6** and **7** were comparatively examined by using an open-aperture Z-scan method in the wavelength range of 1400–2400 nm, where one-photon absorption contributions are negligible (Fig. 8). The TPA cross-section maxima ( $\delta^{(2)}_{\text{max}}$ ) were determined to be 180 GM for **8Zn** ( $\lambda_{\text{ex}} = 1600$  nm), 340 GM for **5Zn** ( $\lambda_{\text{ex}} = 1600$  nm), 980 GM for **6** ( $\lambda_{\text{ex}} = 1700$  nm) and 580 GM for **7** ( $\lambda_{\text{ex}} = 2300$  nm), respectively. The TPA value of **8Zn** is larger than that of usual porphyrin monomer (<100 GM),<sup>28</sup> which can be ascribed to the  $\pi$ -extended structure. The observed larger TPA value of **6** as compared with **7** again indicates its extended  $\pi$ -conjugation.

## Conclusions

In summary, the oxidations of porphyrins bearing strongly electron-withdrawing substituents at the 5-position with DDQ and  $\text{FeCl}_3$  resulted in the selective fusion of the 10- and 20-aryl groups at the 12- and 18-positions, indicating that the electron-withdrawing group dictated the unique selectivity. Doubly phenylene-fused *meso*-chloroporphyrin **2c** was converted to quadruply phenylene-fused *meso-meso*,  $\beta$ - $\beta$ ,  $\beta$ - $\beta$  triply linked Zn(II)-diporphyrin **6**, which displays red-shifted absorption bands in the near-infrared region, smaller optical and electrochemical HOMO–LUMO gap, and a larger TPA value as compared to the usual *meso-meso*,  $\beta$ - $\beta$ ,  $\beta$ - $\beta$  triply linked Zn(II)-diporphyrin **7**. These features may be ascribed to its extended  $\pi$ -conjugation and pseudo  $20\pi$ -antiaromatic contribution. More elaborate systems based on multiply phenylene-fused porphyrins are now actively being pursued in our laboratory.

## Acknowledgements

The work at Kyoto University was supported by Grants-in-Aid from MEXT (No.: 25107002 “Science of Atomic Layers”), from JSPS (No.: 25220802 (Scientific Research (S)), 24685007 (Young Scientists (A)), 26620081 (Exploratory Research)), and from ACT-C, JST. N. F. acknowledges a JSPS Fellowship for Young Scientists. H. Y. acknowledges Kansai Research Foundation for Technology Promotion and Asahi Glass Foundation for financial support. The work at Yonsei University was supported by Global Research Laboratory (2013K1A1A2A02050183) through the National Research Foundation of Korea (NRF) funded by the Ministry of Science, ICT (Information and Communication Technologies) and Future Planning. The quantum calculations of ACID and NICS values were performed using the super-computing resources of the Korea Institute of Science and Technology Information (KISTI).

## Notes and references

- (a) H. L. Anderson, *Chem. Commun.*, 1999, 2323; (b) M. Craça, H. Vicente, L. Jaquinod and K. M. Smith, *Chem. Commun.*, 1999, 1771; (c) J. R. Reimers, N. S. Hush and M. J. Crossley, *J. Porphyrins Phthalocyanines*, 2002, **6**, 795; (d) S. Fox and R. W. Boyle, *Tetrahedron*, 2006, **62**, 10039; (e) N. Aratani, D. Kim and A. Osuka, *Chem.-Asian J.*, 2009, **4**, 1172; (f) C. Jiao and J. Wu, *Synlett*, 2012, **23**, 171; (g) J. P. Lewtak

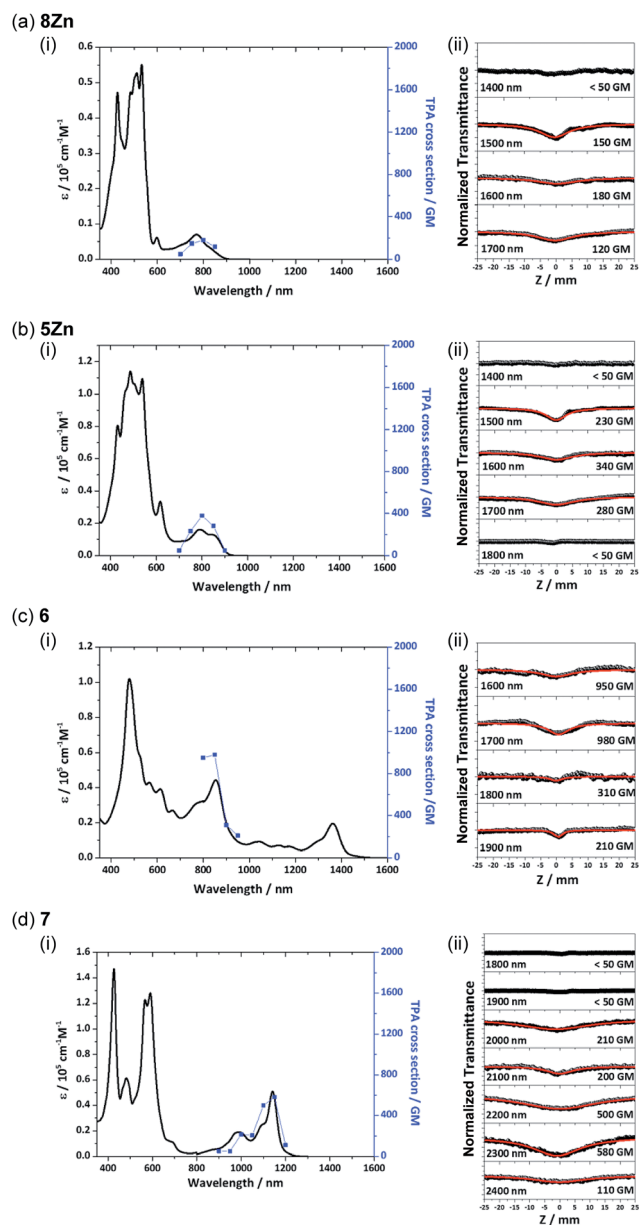
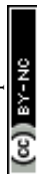


Fig. 8 (i) One-photon absorption (black) and TPA spectra (blue) and (ii) Z-scan curves of (a) **8Zn**, (b) **5Zn**, (c) **6** and (d) **7**. The TPA spectra are displayed at  $\lambda_{\text{ex}}/2$  for comparison with the OPA spectra.



- and D. T. Gryko, *Chem. Commun.*, 2012, **48**, 10069; (h) A. M. V. M. Pereira, S. Richeter, C. Jeandon, J.-P. Gisselbrecht, J. Wytko and R. Ruppert, *J. Porphyrins Phthalocyanines*, 2012, **16**, 464; (i) H. Mori, T. Tanaka and A. Osuka, *Chem.-Asian J.*, 2013, **1**, 2500; (j) T. Tanaka and A. Osuka, *Chem. Soc. Rev.*, 2015, **44**, 943.
- 2 (a) S. Fox and R. W. Boyle, *Chem. Commun.*, 2004, 1322; (b) D.-M. Shen, C. Liu and Q.-Y. Chen, *Chem. Commun.*, 2005, 4982; (c) S. Hayashi, Y. Matsubara, S. Eu, H. Hayashi, T. Umeyama, Y. Matano and H. Imahori, *Chem. Lett.*, 2008, **37**, 846; (d) T. D. Lash, B. E. Smith, M. J. Melquist and B. A. Godfrey, *J. Org. Chem.*, 2011, **76**, 5335; (e) Y. Mitsushige, S. Yamaguchi, B. S. Lee, Y. M. Sung, S. Kuhri, C. A. Schierl, D. M. Guldi, D. Kim and Y. Matsuo, *J. Am. Chem. Soc.*, 2012, **134**, 16540; (f) T. Ishizuka, Y. Saegusa, Y. Shiota, K. Ohtake, K. Yoshizawa and T. Kojima, *Chem. Commun.*, 2013, **49**, 5939.
  - 3 (a) A. Nakano, N. Aratani, H. Furuta and A. Osuka, *Chem. Commun.*, 2001, 1920; (b) A. K. Sahoo, S. Mori, H. Shinokubo and A. Osuka, *Angew. Chem., Int. Ed.*, 2006, **45**, 7972; (c) N. Fukui, H. Yorimitsu, J. M. Lim, D. Kim and A. Osuka, *Angew. Chem., Int. Ed.*, 2014, **53**, 4395; (d) N. Fukui, S. Arai, H. Shinokubo, H. Yorimitsu and A. Osuka, *Heterocycles*, 2015, **90**, 252.
  - 4 (a) H. S. Gill, M. Harmjanz, J. Satamaria, I. Finger and M. J. Scott, *Angew. Chem., Int. Ed.*, 2004, **43**, 485; (b) J. H. Heo, T. Ikeda, J. M. Lim, N. Aratani, A. Osuka and D. Kim, *J. Phys. Chem. B*, 2010, **114**, 14528; (c) K. Ota, T. Tanaka and A. Osuka, *Org. Lett.*, 2014, **16**, 2974.
  - 5 N. Fukui, W.-Y. Cha, S. Lee, S. Tokuji, D. Kim, H. Yorimitsu and A. Osuka, *Angew. Chem., Int. Ed.*, 2013, **52**, 9728.
  - 6 Q. Chen, Y.-Z. Zhu, Q.-J. Fan, S.-C. Zhang and J.-Y. Zheng, *Org. Lett.*, 2014, **16**, 1590.
  - 7 Y. Matano, K. Matsumoto, Y. Terasaka, H. Hotta, Y. Araki, O. Ito, M. Shiro, T. Sasamori, N. Tokitoh and H. Imahori, *Chem.-Eur. J.*, 2007, **13**, 891.
  - 8 Crystallographic data for **2e**:  $C_{64}H_{67}N_5O_2Ni \cdot 2CHCl_3$ , orthorhombic, space group *Pbcn* (no. 60),  $a = 11.0983(14)$ ,  $b = 34.992(5)$ ,  $c = 32.965(4)$  Å,  $V = 12802(3)$  Å<sup>3</sup>,  $T = 123$  K,  $Z = 8$ ,  $R_1 = 0.0921$  ( $I > 2\sigma(I)$ ),  $R_w = 0.2889$  (all data), GOF = 1.047. CCDC number: 1433487. Crystallographic data for **2f**:  $C_{74}H_{77}N_4OPNi \cdot C_6H_5CH_3 \cdot 1.5CH_3CH_2OH$ , monoclinic, space group *P2<sub>1</sub>/n* (no. 14),  $a = 12.3714(16)$ ,  $b = 28.233(3)$ ,  $c = 41.360(6)$  Å,  $\beta = 96.168(4)^\circ$ ,  $V = 14363(3)$  Å<sup>3</sup>,  $T = 123$  K,  $Z = 8$ ,  $R_1 = 0.0739$  ( $I > 2\sigma(I)$ ),  $R_w = 0.2350$  (all data), GOF = 1.036. CCDC number: 1433489. Crystallographic data for **3**:  $C_{62}H_{69}N_5O_2Ni \cdot C_6H_5CH_3$ , triclinic, space group *P $\bar{1}$*  (no. 2),  $a = 14.734(6)$ ,  $b = 20.554(8)$ ,  $c = 20.788(9)$  Å,  $\alpha = 90.073(8)$ ,  $\beta = 103.209(15)$ ,  $\gamma = 109.518(5)^\circ$ ,  $V = 5756(4)$  Å<sup>3</sup>,  $T = 123$  K,  $Z = 2$ ,  $R_1 = 0.1419$  ( $I > 2\sigma(I)$ ),  $R_w = 0.3713$  (all data), GOF = 1.097. CCDC number: 1433488.
  - 9 Y. Fang, D. Koszelewski, K. M. Kadish and D. T. Gryko, *Chem. Commun.*, 2014, **50**, 8864.
  - 10 O. Yamane, K.-i. Sugiura, H. Miyasaka, K. Nakamura, T. Fujimoto, K. Nakamura, T. Kaneda, Y. Sakata and M. Yamashita, *Chem. Lett.*, 2004, **33**, 40.
  - 11 (a) M. Gałęzowski and D. T. Gryko, *J. Org. Chem.*, 2006, **71**, 5942; (b) K. Oda, S. Hiroto and H. Shinokubo, *Chem. Lett.*, 2014, **43**, 1444.
  - 12 M. J. Frisch, *et al.*, *Gaussian 09, Revision A.02*, Gaussian, Inc., Wallingford, CT, 2009. The full list of the authors is given in ESI.†
  - 13 M. Grzybowski, K. Skonieczny, H. Butenschön and D. T. Gryko, *Angew. Chem., Int. Ed.*, 2013, **52**, 9900.
  - 14 A. G. Hyslop, M. A. Kellett, P. M. Iovine and M. J. Therien, *J. Am. Chem. Soc.*, 1998, **120**, 12676.
  - 15 (a) J. M. Murphy, X. Liao and J. F. Hartwig, *J. Am. Chem. Soc.*, 2007, **129**, 15434; (b) H. Wu and J. Jr. Hynes, *Org. Lett.*, 2010, **12**, 1192; (c) K. Fujimoto, H. Yorimitsu and A. Osuka, *Org. Lett.*, 2014, **16**, 972.
  - 16 (a) M. F. Semmelhack, P. M. Helquist and L. D. Jones, *J. Am. Chem. Soc.*, 1971, **93**, 5908; (b) M. Kitano, J. Sung, K. H. Park, H. Yorimitsu, D. Kim and A. Osuka, *Chem.-Eur. J.*, 2013, **19**, 16523.
  - 17 (a) A. Tsuda, H. Furuta and A. Osuka, *Angew. Chem., Int. Ed.*, 2000, **39**, 2549; (b) A. Tsuda and A. Osuka, *Science*, 2001, **293**, 79; (c) A. Tsuda, H. Furuta and A. Osuka, *J. Am. Chem. Soc.*, 2001, **123**, 10304; (d) T. Ikeue, N. Aratani and A. Osuka, *Isr. J. Chem.*, 2005, **45**, 293; (e) M. Kamo, A. Tsuda, Y. Nakamura, N. Aratani, K. Furukawa, T. Kato and A. Osuka, *Org. Lett.*, 2003, **5**, 2079; (f) T. Tanaka, Y. Nakamura and A. Osuka, *Chem.-Eur. J.*, 2008, **14**, 204.
  - 18 Crystallographic data for **6**:  $C_{124}H_{130}N_8Zn_2 \cdot 2C_5H_5N \cdot 3C_6H_5CH_3 \cdot CH_3CN$ , triclinic, space group *P $\bar{1}$*  (no. 2),  $a = 10.0013(12)$ ,  $b = 14.5831(10)$ ,  $c = 24.366(4)$  Å,  $\alpha = 75.428(16)$ ,  $\beta = 87.017(19)$ ,  $\gamma = 71.26(2)^\circ$ ,  $V = 3255.6(8)$  Å<sup>3</sup>,  $T = 123$  K,  $Z = 1$ ,  $R_1 = 0.0531$  ( $I > 2\sigma(I)$ ),  $R_w = 0.1531$  (all data), GOF = 1.018. CCDC number: 1433486.
  - 19 The MPD of **6** is defined by the 48 core atoms consisting of eight pyrrole units and eight methine carbons.
  - 20 (a) D. Geuenich, K. Hess, F. Köhler and R. Herges, *Chem. Rev.*, 2005, **105**, 3758; (b) R. Herges and D. Geuenich, *J. Phys. Chem. A*, 2001, **105**, 3214.
  - 21 (a) Z. Chen, C. S. Wannere, C. Corminboeuf, R. Puchta and P. v. R. Schleyer, *Chem. Rev.*, 2005, **105**, 3842; (b) P. v. R. Schleyer, C. Maerker, A. Dransfeld, H. Jiao and N. J. R. v. E. Hommes, *J. Am. Chem. Soc.*, 1996, **118**, 6317.
  - 22 (a) Y. Inokuma, N. Ono, H. Uno, D. Y. Kim, S. B. Noh, D. Kim and A. Osuka, *Chem. Commun.*, 2005, 3782; (b) V. V. Diev, K. Hanson, J. D. Zimmerman, S. R. Forrest and M. E. Thompson, *Angew. Chem., Int. Ed.*, 2010, **49**, 5523; (c) N. K. S. Davis, A. L. Thompson and H. L. Anderson, *Org. Lett.*, 2010, **12**, 2124; (d) J. Luo, S. Lee, M. Son, B. Zheng, K.-W. Huang, Q. Qi, W. Zeng, G. Li, D. Kim and J. Wu, *Chem.-Eur. J.*, 2015, **21**, 3708.
  - 23 K. Fujimoto, H. Yorimitsu and A. Osuka, *Chem.-Eur. J.*, 2015, **21**, 11311.
  - 24 A. Tsuda, H. Furuta and A. Osuka, *J. Am. Chem. Soc.*, 2001, **123**, 10304.
  - 25 H. S. Cho, D. H. Jeong, S. Cho, D. Kim, Y. Matsuzaki, K. Tanaka, A. Tsuda and A. Osuka, *J. Am. Chem. Soc.*, 2002, **124**, 14642.



- 26 N. J. Turro, *Modern Molecular Photochemistry*, University Science Books, Sausalito, CA, 1991.
- 27 (a) A. Nowak-Król, M. Grzybowski, J. Romiszawski, M. Drobizhev, G. Wicks, M. Chotkowski, A. Rebane, E. Górecka and D. T. Gryko, *Chem. Commun.*, 2013, **49**, 8368; (b) J. Schmitt, V. Heitz, A. Sour, F. Bolze, H. Ftouni, J.-F. Nicoud, L. Flamigni and B. Ventura, *Angew. Chem., Int. Ed.*, 2015, **54**, 169.
- 28 (a) T. Ikeda, N. Aratani and A. Osuka, *Chem.-Asian J.*, 2009, **4**, 1248; (b) M. Drobizhev, A. Karotki, M. Kruk and A. Rebane, *Chem. Phys. Lett.*, 2002, **355**, 175.

